LUND UNIVERSITY
Faculty of Science

Calibration measurements in a catalysis reaction chamber using thermographic phosphors

Hanna Karlsson

Thesis submitted for the degree of Bachelor of Science
Project duration: 2 months

Supervised by Johan Zetterberg and Fahed Abou Nada

Department of Physics
Division of Combustion Physics
May 2015

Lund Reports on Combustion Physics, LRCP-186
ISRN LUTFD2/TPC-186-SE
ISSN 1102-8718
Lund, Sweden, May 2015
Hanna Karlsson
Division of Combustion Physics
Department of Physics
Lund University
P.O. Box 118
S-221 00 Lund, Sweden

Populärvetenskaplig sammanfattning

Kanelbulle och katalysator: Temperaturerna som förändrar världen

Temperatur är något som de flesta av oss talar om dagligen. Det må handla om vädrets föränderlighet eller värmepannans oförmåga att värma upp huset; oavsett vad så är temperatur en faktor som diskuteras. För en katalysator i en kemisk omvandling är korrekt temperatur avgörande, och kan spela stor roll för framtidens utvecklingar inom såväl industri som samhället i stort.

Föreställ dig en fredag eftermiddag i köket då jobbet precis har blivit färdigt för dagen. Det är dags för fredagsmys och du är sugen på en löjligt god kanelbulle, helt i enlighet med den som Per Morberg tillagade igår kväll i ”Vad blir det för mat?”. Det första du gör är att sätta på ugnen på rätt temperatur enligt receptet, men så slås du av en tanke. Hur kan man vara säker på att temperaturen i ugnen faktiskt är den som vredet utanpå visar? Om temperaturen inte är korrekt kommer den löjligt goda kanelbullen att bli förstörd och oaptitlig, och en förstörd och oaptitlig bulle är inte det man är sugen på en fredagskväll.

Att använda en katalysator i en kemisk omvanlding kan på sätt och vis liknas vid att baka kanelbullar. En katalysator är ett ämne som påskyndar en omvandling mellan andra ämnen till ett nytt ämne, liksom jästen i bulldegen. Allt vetemjöl, socker och kanel skulle inte kunna bli den där goda bullen lika enkelt om jästen inte fanns där och snabbade på bakningen genom att göra degen luftig. För liksom jästen i brödet så är en katalysator i en kemisk process helt beroende av vilka temperaturer som används, och det nya ämnet kan inte bildas lika snabbt och effektivt utan katalysatorn. Om temperaturen är fel kommer därför det nya ämnet antingen att inte skapas alls, eller i mindre utsträckning än vad det hade kunnat göra.

Katalysatorer används idag i någon form i ungefär 90% av alla kemiska produkter som produceras och det är därför viktigt att ha god kunskap om de processer som en katalysator kan sätta igång. Eftersom en katalysator börjar skapa det nya ämnet först vid en given temperatur så är det viktigt att veta vilken temperatur som råder där man vill att den kemiska processen skall äga rum. Detta kan man göra genom att studera ljus från vissa material kallade termografiska fosforer, vilka skickar ut ljus som beror av materialets egen temperatur. Genom att i förväg veta vilket sorts ljus som skickas ut vid en specifik temperatur kan man på så sätt bestämma temperaturen i katalysatorns omgivning, den så kallade mätkammaren.

I detta arbete har det visat sig att temperaturen i mätkammaren är högre än vad man tidigare trott, och att den dessutom varierar beroende på var i mätkammaren som mätningarna utförts. Detta innebär att det nu är möjligt att vara mer säker på vilka temperaturer som faktiskt råder i mätkammaren, och att det spelar stor roll var i kammaren som man placerar katalysatorn och ämnena som ska omvandlas. I förlängningen kommer det därför att innebära att mätningarna kan genomföras snabbare utan att man behöver undra vilken temperatur det är i mätkammaren, samt att nya katalysatorer kan utvecklas och undersökas med större precision. Precis liksom att du får löjligt goda kanelbullar en fredagkväll, kommer världen att få fler och bättre kemiska produkter att använda i alla delar av samhället. Allt tack vare att någon kollade vilka temperaturer som egentligen fanns där man verkligen behövde veta det.

Abstract

Accurate temperature measurements using thermocouples inside a catalysis reaction chamber is problematic due to the difficulties to attach the thermocouple to the catalysis sample. It is also of interest to accurately know the pressure inside the reaction chamber. In this work, thermographic phosphors have been utilized in order to determine the temperatures occurring inside a catalysis reaction chamber for typical catalysis measurement environments, and a pressure calibration has been performed. The phosphor was coated on top of the sample holder inside the reaction chamber and on phantom samples imitating real catalytic samples. The results show that the measured temperatures are higher at all locations on the sample holder compared to the temperature readings of the thermocouple, and that the heat transfer to the phantom samples can be said to be fairly efficient. The results also shows that the pressure inside the chamber changes quadratically with a change in flow through the chamber.

List of abbreviations

FTIR	Fourier transform infrared spectrometry
HPXPS	High-pressure X-ray photoemission spectroscopy
LIF	Laser-induced fluorescence
MFC	Mass flow controllers
MS	Mass spectrometry
PLIF	Planar laser-induced fluorescence
PMT	Photomultiplier tube
STM	Scanning tunneling microscopy
UHV	Ultrahigh vacuum
UV	Ultra violet

Contents

1 Introduction

A catalyst is a substance that accelerates a certain chemical process while not being consumed itself. The chemical process occurring on the surface of the catalyst will depend on the temperature, while the production of the new substances depends on the gas flow used. Catalytic reactions are present in several different research areas, such as minimizing damaging gases as final products in combustion events [1] or in production of fermentable sugars as a bio fuel [2]. A model of a catalytic process can be seen in figure 1. Transition metals are often used in catalytic events and have therefore been studied extensively, where the main focus of the studies lies on the gas-surface interactions. Several studies have been done on catalysts in ultrahigh vacuum (UHV), but in reality catalysts are mainly operated at higher pressures with specific gas compositions. At higher pressures the number of gas molecules interacting with the surface increases significantly, influencing the surface structure and thereby the catalytic activity. The gas flow through the reactor, where the catalyst is placed, will also have an impact on the gas distribution and composition surrounding the sample and therefore affects the sample surface. It is thus necessary to investigate the behaviour of the catalysis process in situ and in the absence of vacuum, which can be done by e.g. ambient scanning tunneling microscopy (STM) [3] and high pressure X-ray photoemission spectroscopy (HPXPS) [4].

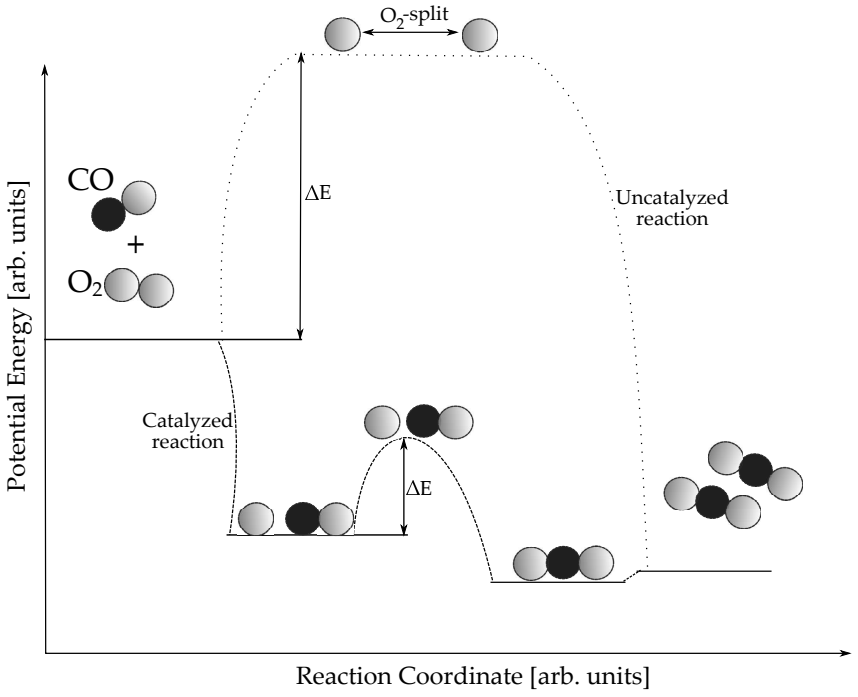

Figure 1: A simplified model of the catalytic process of CO oxidation. It is not possible for two reactants to react due to a potential energy barrier, but the presence of a catalyst makes it possible. The process results in a final product without the catalyst being consumed.

The efficiency of a catalyst is determined by analysing the resulting products from the reaction, which is often done by using mass spectrometry (MS) [5]. MS allows for multi-species measurements inside a reactor, and is generally positioned at the gas outlet of the reaction chamber. One of the major drawbacks of MS is its position, since it normally measures the species at a location distant from the actual reaction. It is also possible to probe the gas close to the sample with MS, but it is inconvenient since it is an intrusive

method and thus can affect both the gas flow and the temperature inside the reaction chamber which alters the final result. An alternative to MS is Fourier transform infrared spectrometry (FTIR) which is a non-intrusive technique based on infrared light scanning the gas of interest. However, FTIR requires a line-of-sight set-up and the output signal is integrated over the entire path which gives a poor spatial resolution [6].

In many cases, it is much more beneficial to use laser based techniques, since they are non-intrusive and provide high spatial and temporal resolution. Parameters that can be measured using laser spectrometry includes, but are not limited to temperature, species concentrations and particle size. Laser-based techniques are frequently used in several different areas of research including cancer research [7] and environmental applications such as monitoring water quality [8]. Some techniques used in different areas of combustion science are laser-induced fluorescence (LIF), laser absorption and multi-photon spectroscopy. LIF is one of the most used laser techniques because of its high sensitivity, good spatial resolution and its ability to probe different molecules [9]. LIF can also be expanded into two dimensions by applying planar laser-induced fluorescence (PLIF), which utilizes the good qualities of LIF in 2D [10].

Accurate temperature measurements are vital when studying catalytic reactions since the reaction rate of the reactants will depend on the temperature. When the kinetic energy of the reactants is increased, the probability for a final product formation will also increase according to the Boltzmann distribution [11]. There are several methods for measuring temperature. A cheap and well-used method for determining the temperature of a system is the use of thermocouples, which are easy to attach and use. Thermocouples are however intrusive, which might change the properties of the measurement object and therefore introduce a systematic error. The effect of the composition of the thermocouple is not negligible when used in catalytic environments, since the thermocouple itself might act as a catalyst [12]. An alternative method for temperature measurements is by the utilization of thermographic phosphors which are accurate, precise, semi-nonintrusive and allows for remote probing.

In this work, efforts have been made to more clearly determine temperatures and pressures inside a catalysis reaction chamber. The pressure inside the chamber was compared to the inlet and outlet pressures at different flows for both argon and nitrogen as flowing gases. We have also determined the temperature on six different locations on the sample holder of the chamber, where the catalysis sample is placed. The temperature was measured at different pressures and flows, with both argon and nitrogen as flowing gases. The temperature measurement was done by coating the cross by a thermographic phosphor and exciting it by means of a pulsed UV-laser. Stainless steel phantom samples was also used in order to resemble catalytic samples, and these were also coated with the phosphor and temperature data could be retrieved.

2 Method

2.1 Experimental Set-up

An experimental setup was constructed as shown in figure 2. The laser used was a Nd:YAG-laser (Quantel Brilliant-B) operating at an repetition rate of 10 Hz and with a pulse length of 6 ns. The fundamental wavelength of the laser corresponds to 1064 nm, but using frequency quadrupling the desired UV-wavelength of 266 nm was achieved. A Pellin-Broca prism is an optical component that creates a 90 ° deflection for the incoming

beam, where the longer wavelengths of the beam will be less deviated compared to shorter wavelengths. This prism was utilized in order to separate the green laser light from the needed UV-light, and the green light was sent into a beam dump absorbing light of a wavelength of 532 nm. In order to stabilize the pulse energy of the laser beam an attenuator was used to allow the laser to run at high pulse energies for a lower pulse-to-pulse variation. After passing through the attenuator, the laser energy was approximately 25.3 $\pm$1.9 μJ per pulse giving a pulse-to-pulse variation of 8 %. An iris was used to create a laser beam 1 mm in diameter while not changing the laser fluence, but due to scattering of the laser light the beam diameter might have been slightly larger. The iris also created a top-hat profile from the Gaussian laser beam profile by cutting off the edges of the beam. To reach the reaction chamber, the beam was directed by two dichroic mirrors (266 nm) onto the sample holder inside the chamber. The second laser mirror blocked the laser light from passing through while allowing the phosphorescence signal to reach a focusing glass lens of focal length 50 mm. The phosphorescence could then be focused into a photomultiplier tube (Hamamatsu H11256-20-NF), passing through an OG-570 long-pass filter and a bandpass interference filter with a center wavelength of 656.3 $\pm$3 nm (Andover Corp. 656FS03). The signal output was fed into an Oscilloscope (LeCroy HDO 6054) using a 50 Ω termination with a 10 Hz collection rate, synchronized to the triggering of the laser. For the pressure measurements only the chamber, the mass-flow controller, the computer software and the vacuum pump were used.

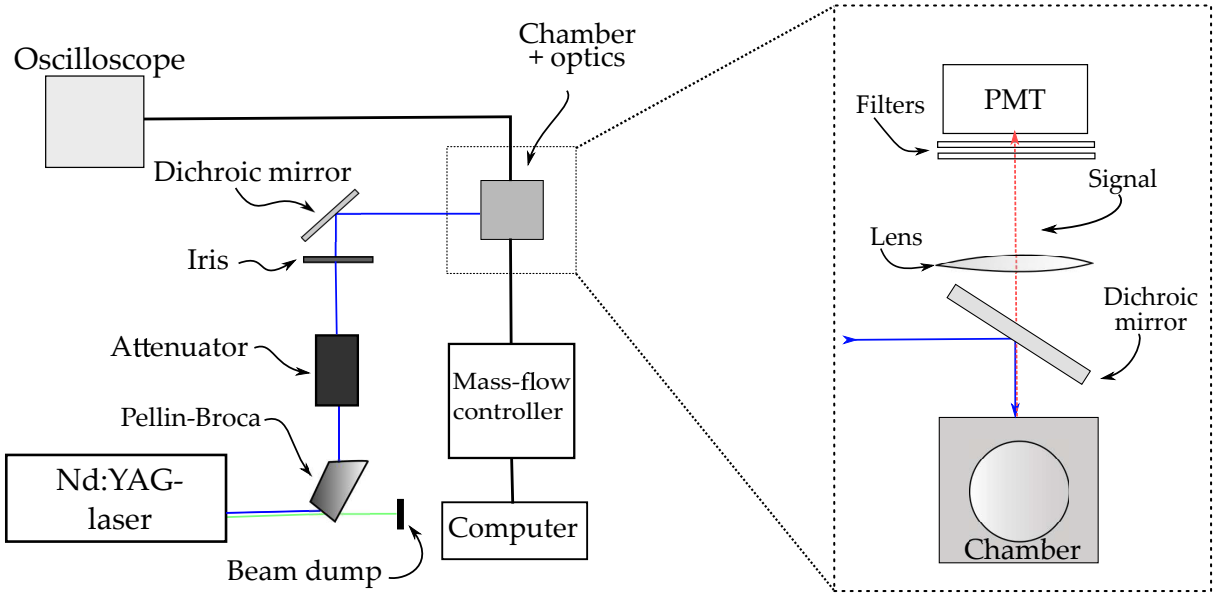

Figure 2: The experimental set-up used for the temperature measurements. The chamber was cooled in order to keep the wall temperature constant. The chamber was also connected to a vacuum pump and a power supply. The pressure measurements were done by only using the chamber, mass-flow controller, vacuum pump (not in figure) and computer software.

2.2 Measuring chamber

The reaction chamber used in the experiment is cube shaped with a volume of approximately 23 cm^3 and four circular windows, three on the sides and one on top. A photograph of the chamber can be seen in Appendix B, figure 25a. The windows used were UV-transparent in order to allow for the laser to pass through the top window properly. Gas flows through the chamber by an inlet at the bottom left of the chamber, and an outlet at

the bottom right. The gas flow is regulated by mass-flow controllers (MFC)(Bronkhorst EL-FLOW) which were calibrated depending on the specific gas. In this experiment argon and nitrogen were used, with a maximum capacity of 480 ml/min and 400 ml/min for Ar and N_2 respectively.

In the middle of the chamber there is a ceramic cross-shaped sample holder connected to a current supply in order to heat it. A photograph of the heating cross can be seen in Appendix B, figure 25b. The heating occurs mainly in the middle of the sample holder, with the heating wire passing from position C5 to position C1 (see figure 4). The temperature of the sample holder is measured by a thermocouple type D at position C5. The chamber is cooled by flowing room temperature water at the edges of the chamber. This is done as to keep the surrounding walls of the chamber at constant temperature. All measurements are performed at sub-atmospheric pressures with a vacuum pump connected to the chamber, and this pressure is kept constant by a pressure regulator attached after the chamber. The pressure was measured by the use of pressure gauges and monitored by a LabView-based computer software.

The main reason why temperature measurements using thermographic phosphors is necessary comes from the composition of the thermocouple used in the reaction chamber where the catalysis measurements are performed. Thermocouples of type C or D are mainly used for catalysis measurements since they are composed of tungsten/rhenium alloys with different composition ratio between the tungsten and rhenium. Other types of thermocouples, such as type K, are nickel alloys which might cause catalytic reactions themselves inside the reaction chamber. The feed-through into the reaction chamber is made from stainless steel which the used type D-thermocouple is not, and the connection with the thermocouple wires creates potential differences which act as a source of error when measuring the temperature. The measured potential difference of the thermocouple is transformed in the computer programme into a temperature using a calibration polynomial for the thermocouple used, and this gives a temperature that differs from the real temperature inside the reaction chamber. Another difficulty when using thermocouples for catalysis measurements is that the thermocouple does not measure the temperature at the location of the catalysis sample, and the possibility to do so is limited.

The flow channels into the catalysis reaction chamber is of a limited size. This is because the mass spectrometer requires that the volume of the chamber is kept as small as possible in order for accurate species measurements. The chamber is also intended for measurements with a low flow of gas, but in reality is used for much higher flows which also causes changes in the chamber pressure. The small flow channels create a pressure drop inside the chamber and thus there is need for accurate pressure calibrations.

2.3 Photomultiplier tube (PMT)

A photomultiplier tube (PMT) is a light detector vacuum tube consisting of an input window, a photocathode, focusing electrodes, dynodes and an anode as shown in figure 3. It makes use of the external photoelectric effect by converting incoming light into electrons through the photocathode. These photoelectrons are then accelerated and focused by the focusing electrodes onto the first of several dynodes where secondary electrons are released. The secondary electrons multiply at each dynode until they are collected by the anode at the end of the tube.

The ratio of output electrons to incident photons onto the input window is called quantum efficiency, and is a probability process dependent on both the mean escape

length of excited electrons and the probability that electrons may be emitted into the vacuum. Since photons of a shorter wavelength are more energetic compared to longer wavelength photons, the quantum efficiency of a PMT will reach a maximum at a slightly shorter wavelength than the peak radiant sensitivity wavelength [13].

The PMT used in this experiment was a Hamamatsu H11526-20-NF photomultiplier tube with a peak sensitivity wavelength of 630 nm and a rise time of 0.57 ns. The PMT was utilized in order to measure the emitted photons from the phosphors and then convert them into an electric signal interpreted by the oscilloscope. The decay time could then be deduced from the measured curve using a fitting algorithm, see sections 2.7 and 2.9.

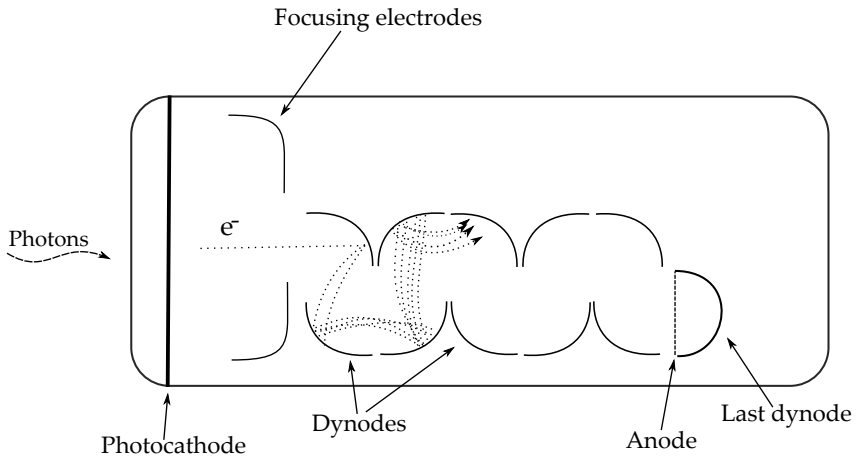

Figure 3: Schematics of a photomultiplier tube. Photons pass through the input window and hits the photocatode, exciting electrons which are emitted into the vacuum. The photoelectrons are accelerated and focused by the focusing electrodes onto the first dynode where secondary electrons are released creating an avalanche effect. The multiplied secondary electrons are then collected by an anode.

2.4 Pressure measurements

The pressure measurements were done at six different set pressures: 10, 50, 100, 200, 500 and 900 mbar, with increasing flows corresponding to 5-100 ml/min for set pressure 10 mbar and 40-480 ml/min for set pressure 900 mbar. The set pressure is the pressure inserted into the LabView software. The pressure regulator used takes this given set pressure and continuously measures it by using a feedback loop, in order to keep it constant. The difference between the set pressure and the measured pressure of the pressure regulator is so small that it can be considered to be equal. Depending on the capacity of the MFC, the maximum flow that could be achieved corresponded to 480 ml/min for argon and 400 ml/min for nitrogen. The flow was increased in steps of 10 ml/min for set pressure 10 mbar and steps of 20 ml/min for the remaining set pressures. One pressure gauge was attached to the test chamber for the entire measurement (photograph of this is shown in Appendix B, figure 26), while the other pressure gauge was first attached to measure the inlet pressure for all pressures and flows and later the outlet pressure for the same conditions. The settings can be seen in table 1.

Table 1: Settings used for the measuring chamber pressure measurements. The step size refers to the increase in flow.

Gas	*Set pressure* [mbar]	*Flow* [ml/min]	*Step size* [ml/min]
Ar, N_2	10	5, 10-100	10
Ar, N_2	50	10, 20-200	20
Ar, N_2	100	10, 20-200	20
Ar, N_2	200	20-400	20
Ar	500, 900	40-480	40
N_2	500, 900	40-400	40

2.5 Temperature measurements

The temperature measurements took place at six different locations on the sample holder (see figure 4), with additional measurements on two different phantom samples S1 and S2 of sizes 4x4 mm and 10x10 mm, respectively, placed in the middle of position C3. Two measurements were done on the 10x10 mm-sample, one at position C3 named S2C3 and another at the edge close to position C2 named S2C2. The set pressures used were 100 mbar and 900 mbar since these are the most probable to be used in forthcoming catalysis measurements. The most commonly used flow in the catalysis measurements is 100 ml/min, which is why this condition was the main focus of these measurements even though 400 ml/min also was investigated. All settings used for the measurements can be seen in table 2.

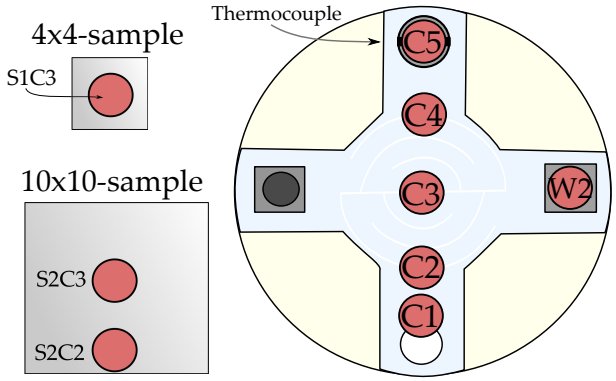

Figure 4: The measurement locations on the sample holder inside the measurement chamber and the two phantom samples. The 4x4-mm sample is referred to as S1C3 and the 10x10-mm sample is called S2 with two different measurement positions, S2C3 and S2C2.

Table 2: Experimental settings used for the temperature measurements. "-" indicates that the measurements were carried out directly on the sample holder. The positions on the sample holder can be seen in figure 4. The absolute pressure is the pressure inside the chamber calibrated according to the pressure measurement results, see section 3.1.

Sample [mm]	*Gas*	*Pressure*[mbar]	*Abs. pressure* [mbar]	*Flows*[ml/min]	*Position*
-	Ar	100	152	100	all
-	Ar	900	911	100	C3, C5
-	Ar	900	941	400	C3, C5
-	N_2	100	142	100	C3, C5
-	N_2	900	910	100	C3
4x4	Ar	100	151	100	S1C3
4x4	Ar	900	911	100	S1C3
4x4	N_2	100	142	100	S1C3
4x4	N_2	900	910	100	S1C3
10x10	Ar	100	152	100	S2C2, S2C3
10x10	Ar	900	911	100	S2C2, S2C3
10x10	N_2	100	142	100	S2C2, S2C3
10x10	N_2	900	910	100	S2C2, S2C3

2.6 Transient temperature measurements

Transient temperature measurements are the most commonly used heating processes in the measurements performed in the reaction chamber, and it is thus vital to monitor the temperature of the phantom sample in a typically applied temperature transient. The temperature in a transient measurement is changed according to a preset profile, including temperature ramp-up, temperature stabilization and temperature ramp-down. The transient measurements were completed using both of the stainless steel phantom samples. Two types of measurements were performed using a set pressure of 100 mbar and a flow of argon of 100 ml/min, giving an absolute chamber pressure of 142 mbar. Two measurements were done for each sample and each setting.

- **Regular ramping: 400-50-400.** Starting at a set temperature of 100 °C and ramping up to 250 °C during 400 s. The temperature 250 °C were kept for 50 s before ramping down again to 100 °C during the time 400 s.
- **Quicker ramping: 60-50-60.** The set temperature start point was 100 °C and the ramp up to 250 °C took 60 s. The temperature was then kept at 250 °C for 50 s before ramping down for 60 s back to 100 °C.

2.7 Thermographic phosphors

In phosphor thermometry one utilizes the phosphorescence of thermographic phosphors in order to measure temperature. A thermographic phosphor is usually composed of a ceramic material doped with rare-earth metal ions that emits phosphorescence when excited with a light source. These rare-earth elements all have similar characteristics, since they have three electrons in the outer shell and only differ in the number of electrons in the 4f-shell. When these rare-earth ions are doped onto a host material, the transitions

occuring in the 4f-shell are unaffected by perturbations in the host and the emissions of the ions will appear as sharp spectral lines [14].

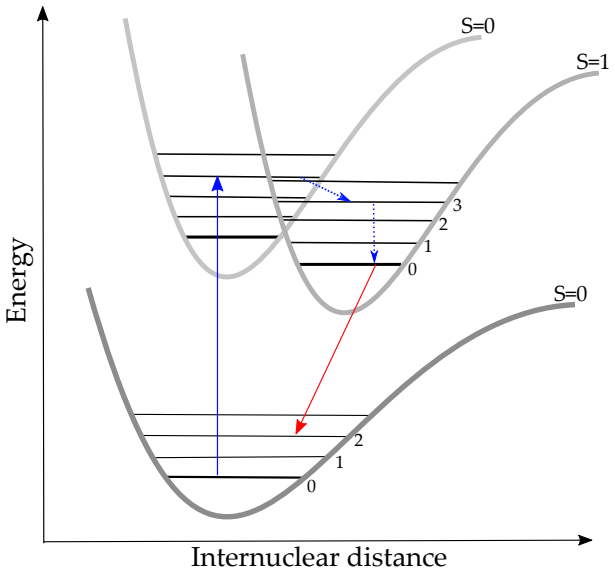

Figure 5: Principle of phosphorescence. The laser light excites phosphor molecules from the singlet ground state to an excited singlet state. Vibrational relaxation (internal conversion) occurs within the excited singlet state, and intersystem crossing follows due to spin-orbit coupling to an excited triplet state. Next, internal conversion within the excited triplet state occurs before de-excitation back to the ground state with emittance of a phosphorescence signal.

The luminescence from the phosphors is based on non-thermal energy conversion into electromagnetic radiation i.e. photons. The decay of the luminescence can be approximately described by a mono-exponential according to

$$I(t) = I_0 e^{-t/\tau} \tag{1}$$

where t is the time, I_0 is the intensity at t=0 and τ is the decay time of the signal. The decay time of luminescence is dependent on the rate of non-radiative (R_{NR}) and radiative (R_R) processes according to

$$\tau = \frac{1}{R_R + R_{NR}} \tag{2}$$

This means that the decay time of the luminescence depends on the rates of non-radiative energy transfer processes, which directly translates to a dependence on temperature of the phosphor. The decay time of the phosphorescence will decrease when the temperature is increased due to a higher rate of non-radiative processes occurring at elevated temperatures [15]. The temperature can also be obtained by the spectral intensity ratio method, which is most common for 2D-measurements and uses the ratio between two or more spectral lines at different wavelengths to determine the temperature. The spectral ratio method is often less accurate compared to the decay time method [14] and is also more influenced by unknown background radiation due to the intensity ratio between the two different wavelength regions [16].

2.8 Sample preparation and Calibration

The phosphor $Mg_3F_2GeO_4$:Mn used in the experiment is a powder phosphor that is highly sensitive from around 350 °C according to the calibration plot seen in figure 6. There were two main reasons for chosing this specific phosphor: one is that the sample holder in the catalysis chamber fluoresces around the wavelength 450 nm, and thus a phosphor with emission in that region would be prone to interferences. Another reason for choosing the specific phosphor was the high temperatures anticipated, and in combination with time constraints the $Mg_3F_2GeO_4$:Mn-phosphor was the best choice.

The phosphor powder was mixed with a magnesium aluminium silicate (HPC) binder which can handle temperatures up to 1500 °C [14]. The sample holder and the samples used were cleaned with alcohol to ensure a clean surface and thus a good adherence to the sample holder surface. The phosphor mixture was sprayed onto the sample holder and the phantom samples in thin layers with drying of the deposited phosphor layer in between sprays as to create a durable and thin layer.

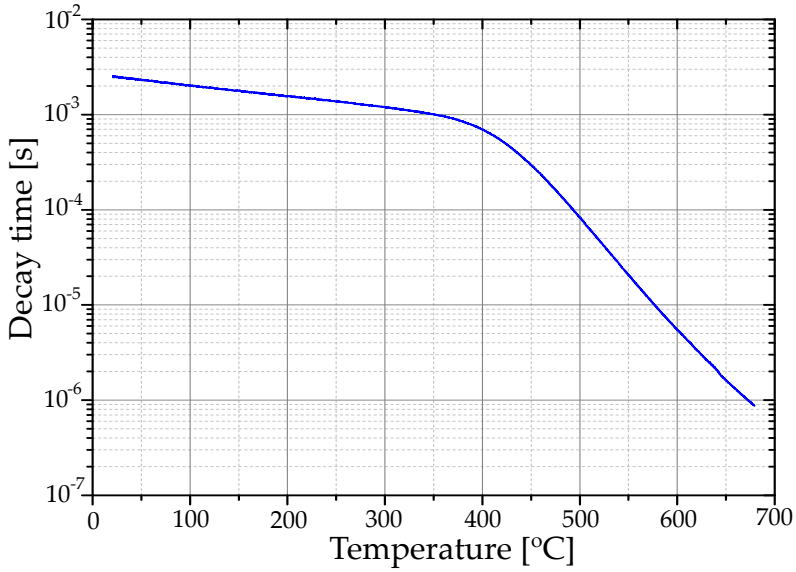

Figure 6: The calibration curve showing the sensitivity of the phosphor $Mg_3F_2GeO_4$:Mn.

The calibration of the phosphor was done by coating a sample connected to three thermocouples (type K) and heating the sample up by means of an electric oven. The same equipment and settings was used in the calibration as in the experimental set-up in order to reduce errors that might emerge due to the implementation of different experimental settings. A Pellin-Broca prism was used in order to only use the 266 nm-wavelength light, and the resulting phosphorescence was focused onto the PMT in the same manner as in the experiment.

2.9 Data evaluation

The phosphorescence decay-signals were saved by the oscilloscope in binary format (.trc format) for the data evaluation process completed using MATLAB. The decay signals were loaded, processed and then fitted with a nonlinear least squares algorithm named Trust-Region reflective algorithm available in the software. In figure 7 the schematics of the processing procedure applied to the decay signal is shown.

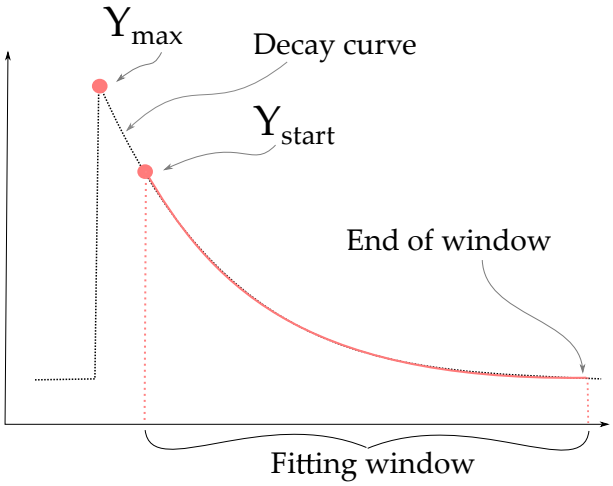

Figure 7: Illustration of the processing procedure applied to the decay curve of the phosphorescence.

The fitting data supplied to the solver fitted a mono-exponential function to the decay signal, which is an approximation since many phosphors display multi-exponential decays. Only the temperature sensitive part of the decay signal was used to extract the decay time, and the temperature sensitive section was defined as data points laying between a cutoff time and an end time. The cutoff time was set at 100 ns after the signal peak and the end time was set at 10% of the signal intensity at the cutoff time. The total time span at which the data was evaluated corresponded to approximately 2.3 decay times (τ). After the calculation of the decay time values of the selected measurement, the decay times were fed to the previously build calibration polynomial to retrieve the corresponding temperatures.

3 Results and discussion

In the following subsections the results of the measurements are presented in combination with discussions and analysis of the results.

3.1 Pressure analysis

The pressure analysis was performed as described in section 2.4 and the results are presented here. In figures 8 - 11 the main results of the pressure analysis are presented. As can be seen in figure 8, the pressure inside the chamber will increase linearly with the flow for a given set pressure. This can be used as to easily determine the chamber pressure when performing a catalysis measurement.

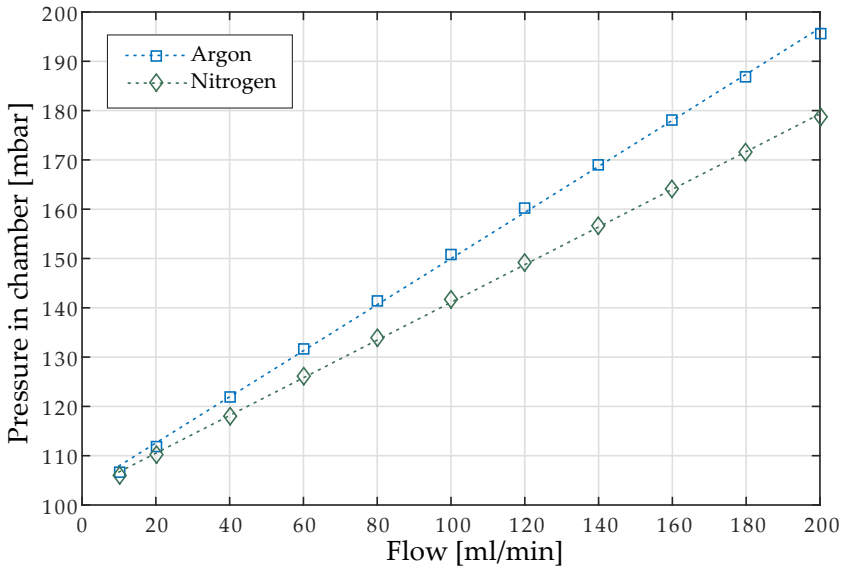

Figure 8: The measured pressure in the chamber for a set pressure of 100 mbar and flows of argon and nitrogen from 10 ml/min to 200 ml/min. The dotted lines corresponds to a linear fit of the data points.

A quadratic curve was fitted to all data points for both gases argon and nitrogen for the same given set pressure. This was done in order to minimize errors for different gases since the result showed that the gas composition has a negligible or no effect on the pressure inside the chamber. The quadratic fit that can be seen in figures 9-11 represent when the measured pressure is fitted to the mean value of the measured inlet pressure and the measured regulator pressure. The reason why the measured chamber pressure was fitted to the mean pressure is because it is a convenient way for the catalysis research group using these results to determine the pressure inside the reaction chamber while performing the actual catalysis measurements. The mean pressure is calculated according to

$$P_M = \frac{P_{in} + P_{reg}}{2} \tag{3}$$

where P_M is the mean pressure of the measured inlet pressure P_{in}, and the pressure measured by the pressure regulator P_{reg}. The regulator pressure can be considered to be constant and equal to the set pressure used in the LabView software. This means that the mean pressure approximately only changes with the inlet pressure, and thus the flow in the measuring chamber. A more accurate result is obtained if one uses the measured outlet pressure in the mean value instead of the measured set pressure, and the difference between using the set pressure or the outlet pressure in the mean value is given in table 3. The reason for not using the measured outlet pressure in the mean value is because it is then required to have another pressure gauge measuring the outlet pressure during all catalysis measurements. This is impractical since the measurement location of the outlet pressure is in close proximity to the location of the MS, which creates a larger volume for the MS to measure and thus the response time of the MS is extended.

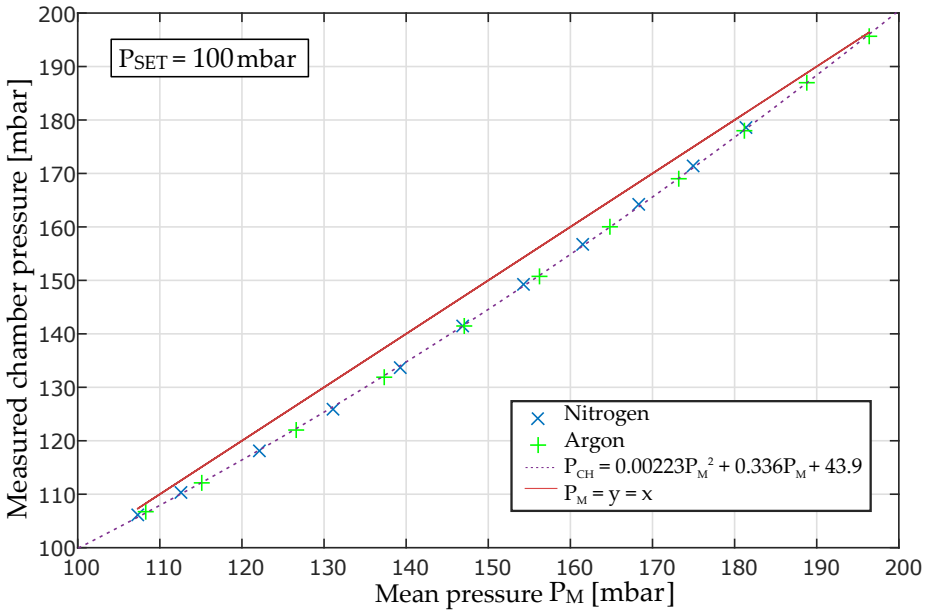

Figure 9: Measured chamber pressures for both argon and nitrogen at a set pressure of 100 mbar. The linear curve corresponds to taking the mean of the inlet pressure and the regulator pressure at each measured inlet pressure which means that the inlet pressure changes with the increase in flow, while the set pressure remains 100 mbar. P_{CH} corresponds to the measured pressure inside the chamber and P_{SET} is the measured set pressure. The maximum absolute difference between the obtained chamber pressures and the linear mean value fit is equal to 5.72 mbar.

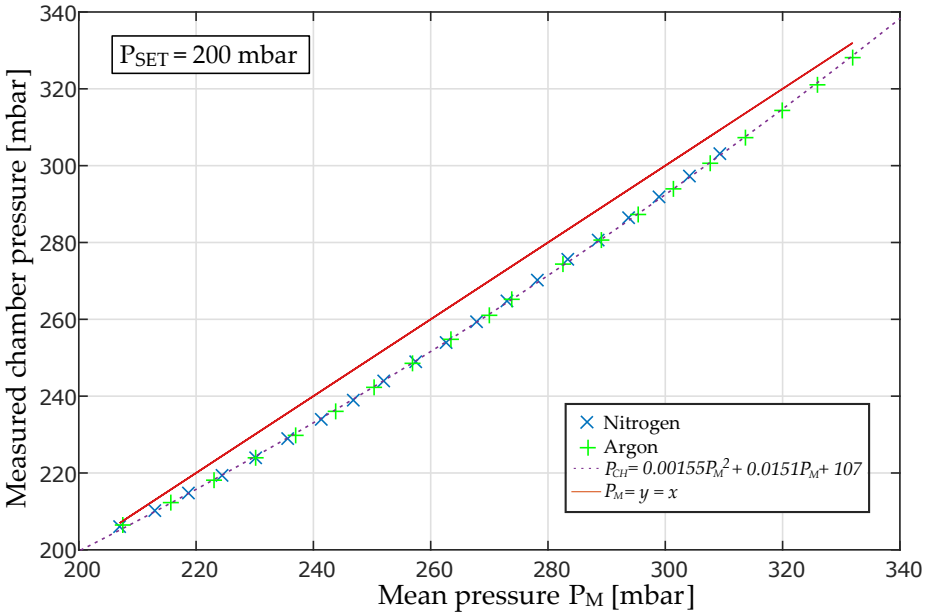

Figure 10: Measured chamber pressures for both argon and nitrogen at a set pressure of 200 mbar. The linear curve corresponds to taking the mean of the inlet pressure and the regulator pressure at each measured inlet pressure which means that the inlet pressure changes with the increase in flow, while the set pressure remains 200 mbar. P_{CH} corresponds to the measured pressure inside the chamber and P_{SET} is the measured set pressure. The maximum absolute difference between the obtained chamber pressures and the linear mean value fit is equal to 8.86 mbar.

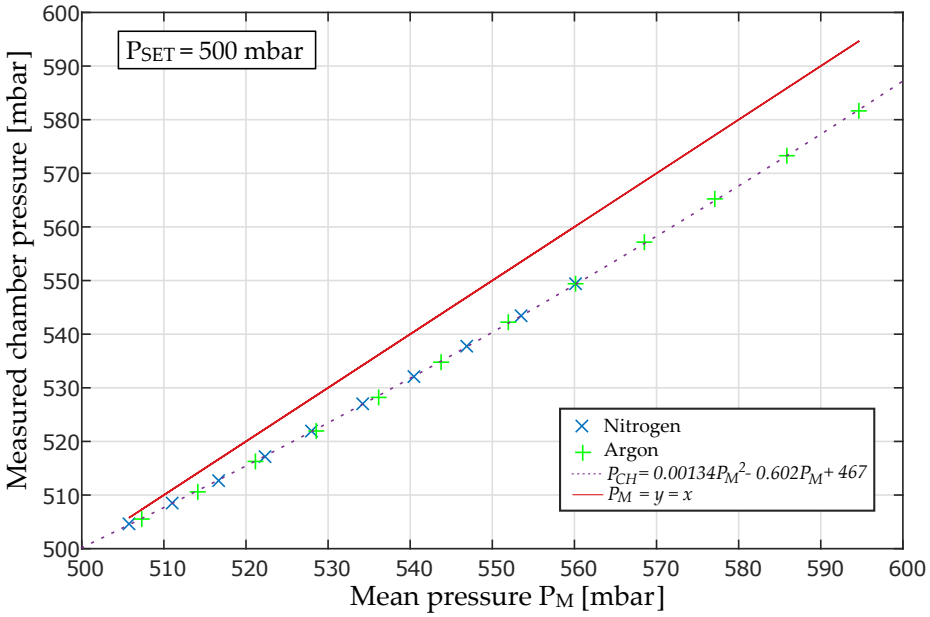

Figure 11: Measured chamber pressures for both argon and nitrogen at a set pressure of 500 mbar. The linear curve corresponds to taking the mean of the inlet pressure and the regulator pressure at each measured inlet pressure which means that the inlet pressure changes with the increase in flow, while the set pressure remains 500 mbar. P_{CH} corresponds to the measured pressure inside the chamber and P_{SET} is the measured set pressure. The maximum absolute difference between the obtained chamber pressures and the linear mean value fit is equal to 13.0 mbar.

For the six set pressures the quadratically fitted curves give good results, but there is always the possibility that other set pressures may be used such as 300 mbar. Since the measured chamber pressure is close to the mean value of the measured regulator pressure and the measured inlet pressure, it can be used as an approximation for estimating the chamber pressure without measuring it as shown in table 3. As can be seen in figures 9-11, the mean pressure corresponds fairly well with the measured chamber pressure and the larger differences occur at elevated pressures with large flows.

Table 3: The difference between using a quadratic fit curve with the mean value of the measured regulator pressure and measured inlet pressure, compared to a quadratic fit curve with mean value of measured outlet pressure and inlet pressure.

Set pressure [mbar]	*Max diff.* [mbar]	*Mean diff.* [mbar]
10	9.4	3.8
50	2.8	1.7
100	1.9	1.2
200	1.8	1.1
500	0.90	0.61
900	0.40	0.29

3.2 Temperature analysis

The temperature measurements were performed according to section 2.5 and the results are presented here, where each data point corresponds to the average of 100 single measurements. The thermocouple reading corresponds to the temperature calculated by the

used LabView software by transforming the measured potential difference of the thermocouple into a temperature, and it was obtained by the standardized calibration polynomial given by the manufacturer of the thermocouple. The thermocouple measures the temperature at position C5 for all measurement positions, and the temperature obtained from the thermocouple is much colder compared to the real temperature inside the reaction chamber as discussed in section 2.2. As expected, the results show that the position C3 on the sample holder has a higher temperature compared to the other positions as shown in figure 12. This is reasonable since the main heating occurs in the middle of the sample holder where position C3 is located. Position W2 has a lower temperature compared to the other positions in the measurements, and this is because the heating wire passes directly from position C5 to position C1 without passing through W2. Positions C2 and C4 can be said to have similar temperatures also. The differences between the positions on the sample holder (excluding W2) as a function of the distance from the center position C3 of the sample holder can be seen in figure 13. It shows that the temperature distribution follows a parabola, where the maximum is at position C3.

Since thermographic phosphors is a rather accurate temperature measurement technique, the standard deviation for temperatures up to 300 °C was about 1 degree and 0.5 degree when the temperature increases beyond 300 °C where the phosphor becomes highly sensitive. Because of this reason, the magnitude of the standard deviation is too small to be visualized and is not shown in the figures.

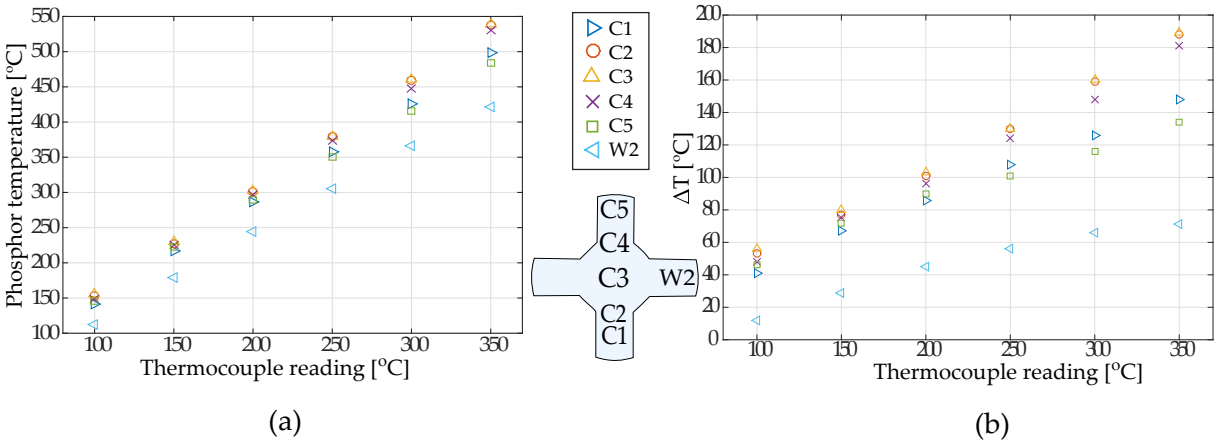

Figure 12: All measured positions on the sample holder at an absolute pressure of 152 mbar and a flow of argon at 100 ml/min. (a) describes the calculated phosphor temperature versus the thermocouple reading, and in (b) ΔT refers to the difference between the phosphor temperature and the thermocouple reading. The approximate positions on the sample holder is also shown in the figure, see figure 4 for further details.

As can be seen in figure 14, the pressure inside the measurement chamber gives no large effect on the temperature measured on the sample holder at position C3. These results are similar for other measurement positions. It is also noticeable that the temperature is lower for a larger flow, where the explanation is that a larger flow means a cooling effect will occur inside the measuring chamber.

There is no noticeable effect on the temperature readings regarding the gas composition, which is shown in figure 15. Both measurements with flow of the two gases shows a linear behaviour with the same temperature differences between the calculated phosphor temperature and the thermocouple temperature. There is one outlier at thermocouple temperature of 350 °C for nitrogen, which can be explained by a miscommunication be-

tween the power supply and the LabView software used to control it. The small differences that do occur could maybe be explained by the different heat capacities of the gases which is equal to 20.85 $J \cdot mol^{-1}K^{-1}$ for argon and 29.12 $J \cdot mol^{-1}K^{-1}$ for nitrogen, even though the effect from the different heat capacities of the gases may be too small to observe.

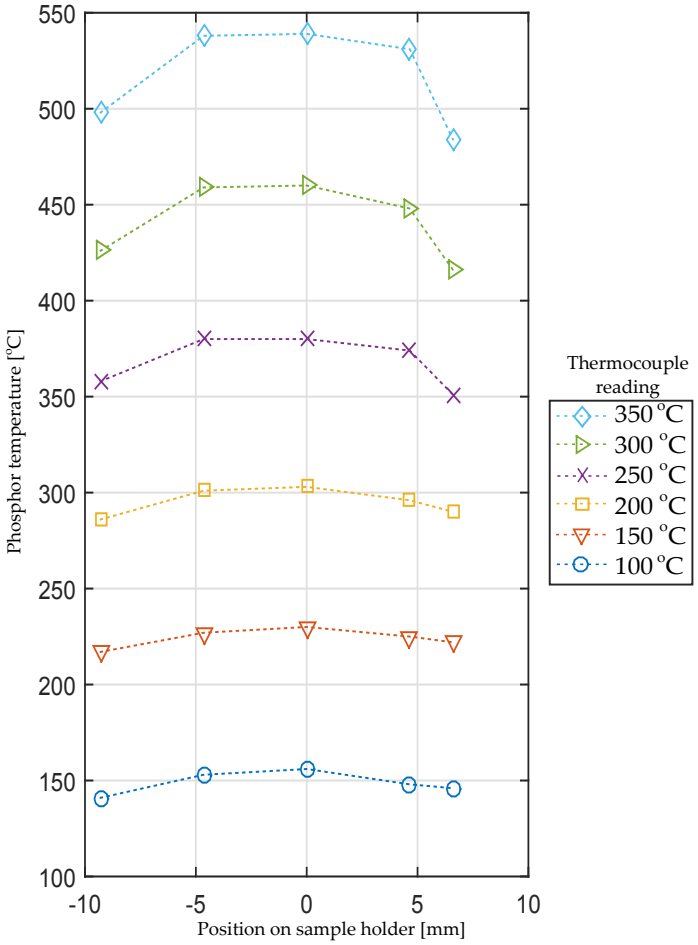

Figure 13: Temperature at positions C1-C5 on the sample holder for thermocouple temperatures from 100 °C to 350 °C. The temperature measurements were done using an absolute pressure of 152 mbar and a flow of argon at 100 ml/min. The temperatures are given as positions on the sample holder where 0 mm corresponds to position C3.

In figure 16 a comparison between the measured temperatures of the samples and the sample holder is made for position C3 and a flow of nitrogen. A direct conclusion from the comparison is that the temperature is lower for the phantom samples compared to the direct measurement on the sample holder. This is due to the heat transfer between the sample holder and the phantom samples, which is difficult to optimize. The thermal conductivity between the sample holder and the phantom samples is not optimum, and heat will be transferred less efficiently to the samples in comparison to only heating up the sample holder. It can also be seen that the larger 10x10-sample has a slightly lower temperature compared to the 4x4-sample, which might be explained by the different mass of the samples. There is only a few degrees difference between the positions S2C2 and S2C3 on the 10x10-sample, and this holds for both gases argon and nitrogen.

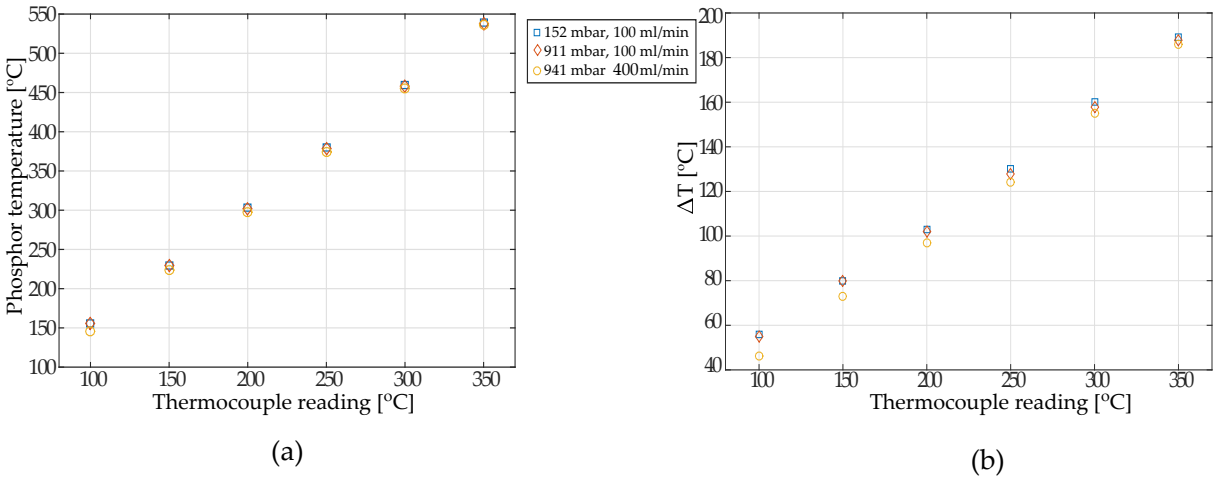

Figure 14: All measurement settings on position C3 for a flow of argon. (a) describes the calculated phosphor temperature versus the thermocouple reading, and in (b) ΔT refers to the difference between the phosphor temperature and the thermocouple reading. The pressure is given as the calibrated chamber pressure.

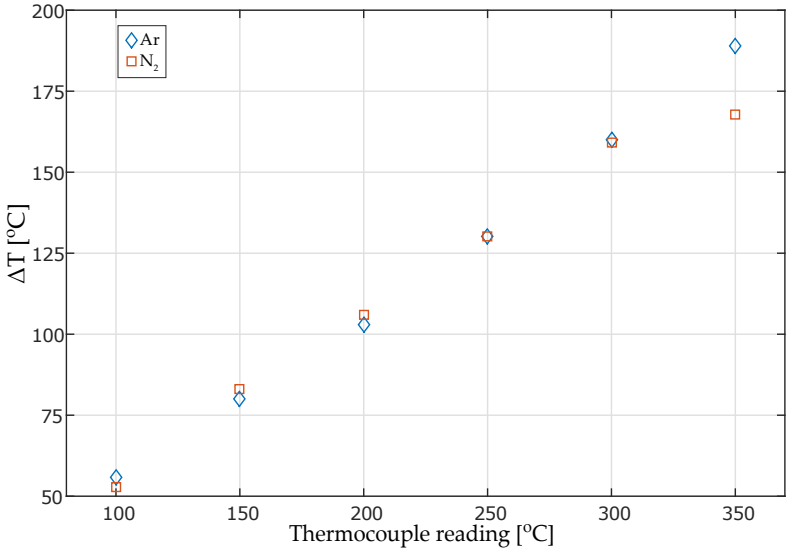

Figure 15: Comparison of phosphor temperatures for flowing argon and nitrogen on position C3 on the sample holder. The measurements were carried out with absolute pressures of 152 mbar (Ar) and 142 mbar (N_2) and a flow of 100 ml/min. ΔT refers to the temperature difference between the phosphor temperature and the thermocouple reading.

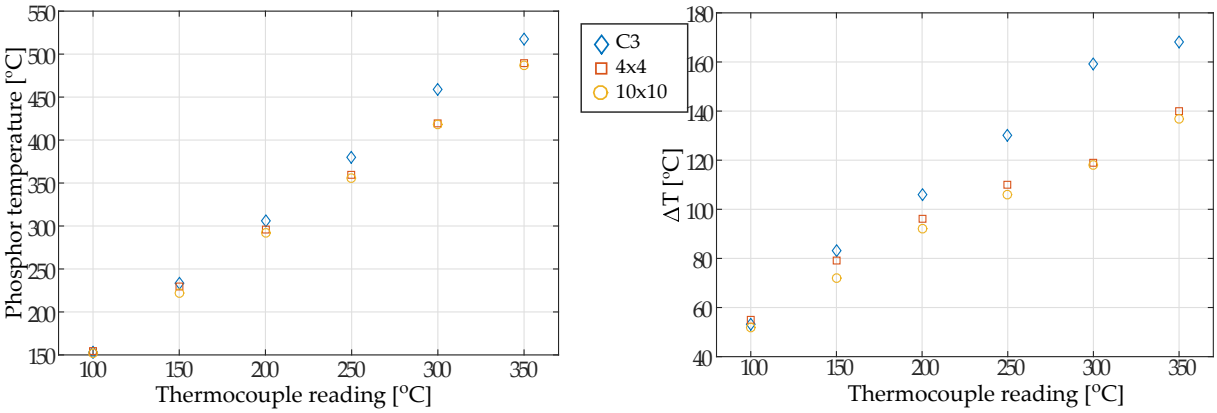

Figure 16: Temperature data at position C3 at an absolute pressure of 141 mbar and a flow of nitrogen at 100 ml/min. ΔT refers to the temperature difference between the phosphor temperature and the thermocouple reading.

3.3 Transient analysis

The transient temperature measurements were completed according to section 2.6 and the results are presented here and in figures 17-18. The results from the transient temperature measurements are rather consistent with the previous temperature measurements; the measured sample temperatures are much higher than the thermocouple readings, and they also follow the temperature ramp-up and ramp-down fairly well. The mean time between the thermocouple's maximum reading and the sample measured maximum temperature is approximately 52 seconds, with a standard deviation of 10 seconds. This holds for both samples and both ramping time periods, which means that 50 s for temperature stabilization is sufficient for catalysis measurements even though the temperature is not as stable as in the previous temperature measurements. A longer temperature stabilization time period would have acquired higher temperatures, but normally the catalyst used in catalysis measurements will become active before the maximum temperature is reached and thus extremely good temperature stabilization may not be necessary.

The measurements done according to the regular ramping time period of 400-50-400 s follows the ramping more accurately than the quick ramping time period, and the explanation for this might be that the sample is given more time to ensure thermal equilibrium in the regular ramping period. When comparing the temperatures obtained for the transient ramping and the regular temperature measurements done on the samples, the difference for the phosphor temperatures at 250 °C is not large and corresponds to a couple of degrees.

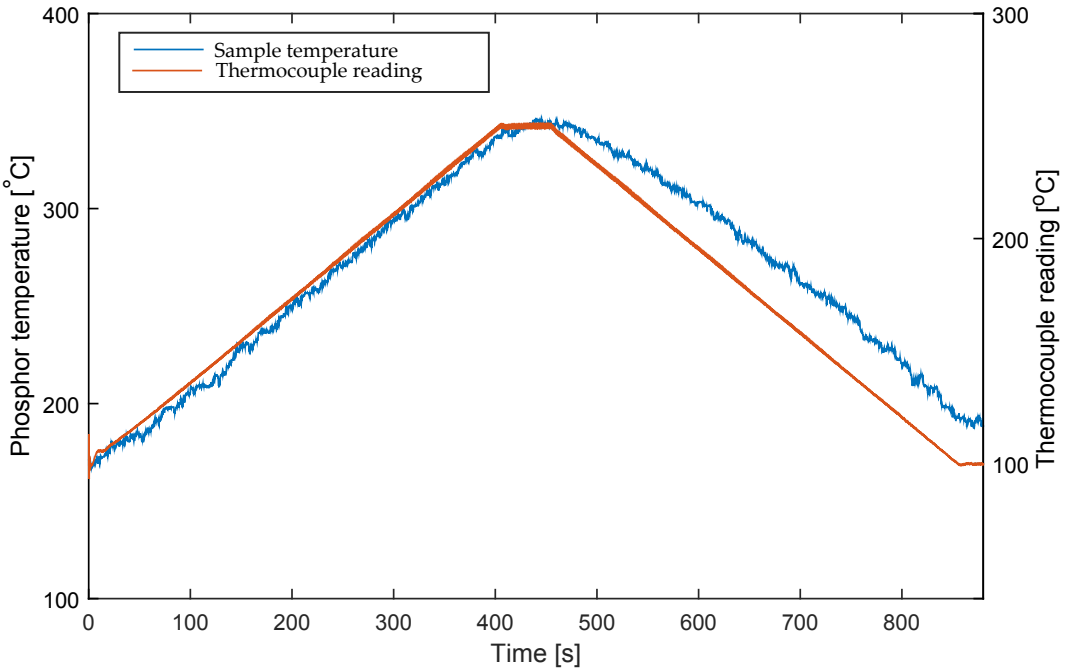

Figure 17: Transient measurement completed on the 4x4-sample according to the regular ramping time period 400-50-400 s. The measurement was done with an absolute pressure of 151 mbar and a flow of argon gas corresponding to 100 ml/min.

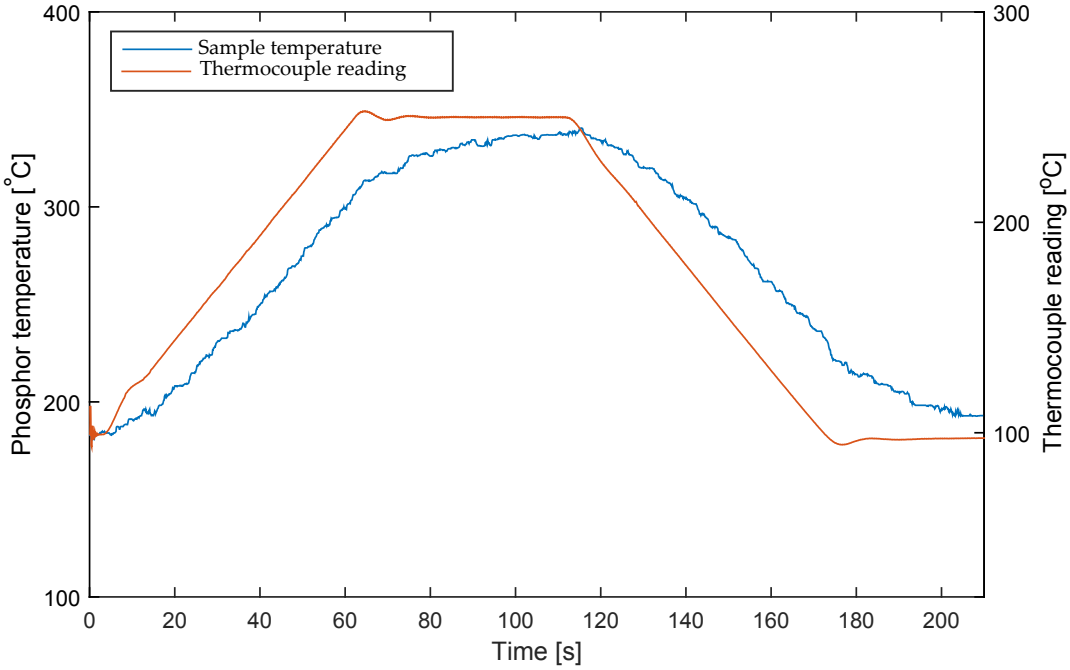

Figure 18: Transient measurement completed on the 4x4-sample according to the quick ramping time period 60-50-60 s. The measurement was done with an absolute pressure of 151 mbar and a flow of argon gas corresponding to 100 ml/min.

4 Summary and outlook

In this thesis, efforts were made to more clearly determine the pressures and temperatures on the sample holder inside a catalysis reaction chamber. The method used for thermometry was thermographic phosphors, which utilizes on the temperature dependent phosphorescence decay time of the phosphor $Mg_3F_2GeO_4$:Mn.

The pressure measurements showed that the measured chamber pressure increases quadratically compared to the mean of the measured regulator pressure and the measured inlet pressure. This pattern holds for six different set pressures, and the results eliminate the use of one pressure gauge used in todays measurements. For pressures not measured in this work, the mean pressure between the set pressure and the inlet pressure works as a good approximation for the chamber pressure. One can also determine the chamber pressure for a given set pressure by studying the chamber pressure as a function of the flow.

The results obtained from the temperature measurements concluded that the position C3 has the highest temperature followed by positions C2 and C4, which is as expected since the main heating of the sample holder occurs in close proximity to these positions. Another conclusion from the temperature measurements is that the gas composition has a negligible or no effect on the temperature of the sample holder, which also holds for the two different pressures used.

The transient temperature measurements performed on both phantom samples showed that the temperature of the samples follows the ramping up and down fairly well. It takes approximately 50 s for the maximum temperature to occur on the sample compared to the thermocouple readings, and there is no major difference between the 4x4mm- and 10x10mm-samples in question of how well the temperature changes with the ramping.

For future implementation, the temperature measurement results have been fitted to linear fits and can be seen in Appendix A, figures 19-23. These linear fits are a suggestion as how to implement the results in reality, and this may be done by using calibration curves in the LabView-based software programme used.

In future works, it would be interesting to determine the lower temperatures with a higher accuracy by using another phosphor than the $Mg_3F_2GeO_4$:Mn-phosphor used here. A phosphor that has a high sensitivity in the region around 100 °C would be a reasonable suggestion, as far as the phosphorescence occurs in a suitable wavelength as to not obtain interference from the sample holder. Even more interesting would be to see the temperature distribution on the sample holder in two dimensions by using thermographic phosphors with the 2D spectral method, and compare it with the results obtained in this work.

Acknowledgements

I would like to thank my supervisors Johan Zetterberg and Fahed Abou Nada for helping and supporting me in this thesis project, they have truly been outstanding supervisors. I also would like to thank the coffee machine at the department of combustion physics for always being there for me and always making me happy in times of trouble.

5 References

[1] Zetterberg J, Blomberg S, Gustafson J, Sun Z W, Li Z S, Lundgren E, Aldén M. *An in situ set up for the detection of CO2 from catalytic CO oxidation by using planar laser-induced fluorescence.* Review of scientific instruments 2012; 83: 053104-1 - 053104-5

[2] Jeong G-T, Kim S-K, Park D-H. *Application of solid-acid catalyst and marine macroalgae Gracilaria verrucosa to production of fermentable sugars.* Bioresource Technology 2015; 181: 1–6

[3] Hendriksen B. L. M,Frenken J. W. M. *CO Oxidation on Pt(110): Scanning Tunneling Microscopy Inside a High-Pressure Flow Reactor.* Phys. Rev. Lett. 2002; 89: 046101-1 - 046101-4

[4] van Rijn R, Balmes O, Resta A, Wermeille D, Westerström R, Gustafsson J, Felici R, Lundgren E, Frenken J. W. M. *Surface structure and reactivity of Pd(100) during CO oxidation near ambient pressures.* Phys. Chem. Chem. Phys. 2011; 13: 13167–13171

[5] Zetterberg J, Blomberg S, Gustafson J, Evertsson J, Zhou J, Adams E C, Carlsson P A, Aldén M, Lundgren M. *Spatially and temporally resolved gas distributions around heterogeneous catalysts using infrared planar laser-induced fluorescence.* Nature Communications 2015; 6: 7076

[6] Snively C. M, Oskarsdottir G, Lauterbach J. *Chemically sensitive parallel analysis of combinatorial catalyst libraries.* Catal. Today 2001; 67: 357-368

[7] Leung P. J, Wu S, Chou C. K, Signorell R. *Investigation of Sub-100 nm Gold Nanoparticles for Laser-Induced Thermotherapy of Cancer.* Nanomaterials 2013; 3: 86-106

[8] Yu X, Li Y, Gu X, Bao J, Yang H, Sun L. *Laser-induced breakdown spectroscopy application in environmental monitoring of water quality: a review.* Environ Monit Assess 2014; 186: 8969-8980

[9] Kohse-Höinghaus K. *Laser Techniques for the Quantitative Detection of Reactive Intermediates in Combustion Systems.* Progress in Energy and Combustion Science 1994; 20: 203-279

[10] Zellner A, Suntz R, Deutschmann O. *Two-Dimensional Spatial Resolution of Concentration Profiles in Catalytic Reactors by Planar Laser-Induced Fluorescence: NO Reduction over Diesel Oxidation Catalysts.* Angew. Chem. 2015; 127: 2691-2693

[11] Blomberg, S. *Planar Laser Induced Fluorescence and High Pressure X-ray Photoelectron Spectroscopy applied to CO oxidation over model catalysts.* 2013. ISBN 9789174734898

[12] Childs P. R. N, Greenwood J. R, Long C. A. *Review of temperature measurement.* Rev. Sci. Instrum. 2000; 71: 2959-2978.

[13] Hamamatsu Photonics K.K. *Photomultiplier tubes: Basics and Applications.* Third edition (2007)

[14] Aldén M, Omrane A, Richter M, Särner G. *Thermographic phosphors for thermometry: A survey of combustion applications.* Progress in Energy and Combustion Science 2011; 37: 422-461

[15] Brübach J, Pflitch C, Dreizler A, Atakan B. *On surface temperature measurements with thermographic phosphors: A review.* Progress in Energy and Combustion Science 2013; 39: 37-60

[16] Seyfried H, Richter M, Aldén M. *Laser-Induced Phosphorescence for Surface Thermometry in the Afterburner of an Aircraft Engine.* AIAA JOURNAL 2007; 45(12):2966-2971

6 Appendix A: Linear temperature fits

The figures 19-21 in this appendix was created in order to see if a linear fit is appropriate to describe the changes in temperature.

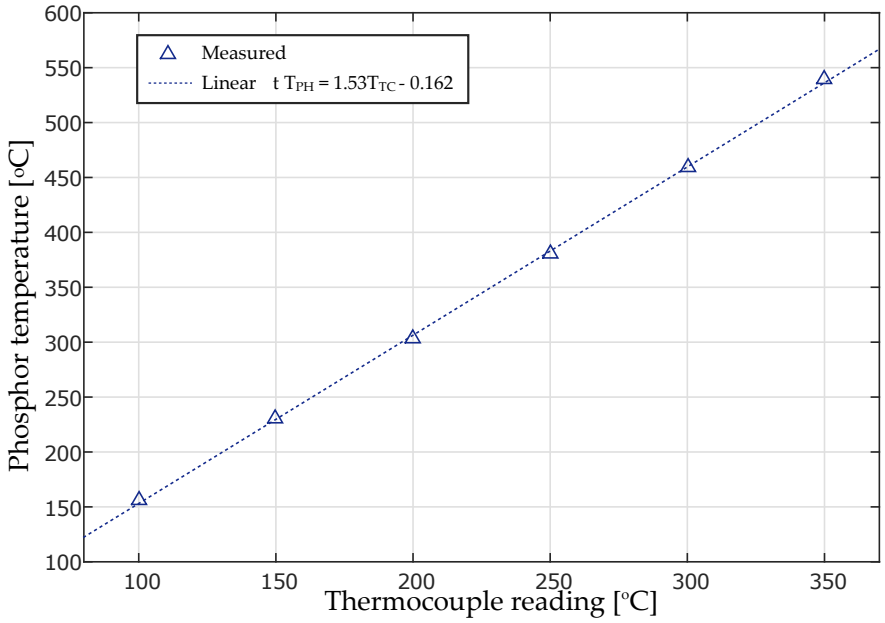

Figure 19: Measured temperature for position C3 and with an absolute pressure of 152 mbar with a flow of argon of 100 ml/min. The dotted line corresponds to the linear fit to the data points. T_{PH} is the temperature of the phosphor and T_{TC} is the thermocouple reading.

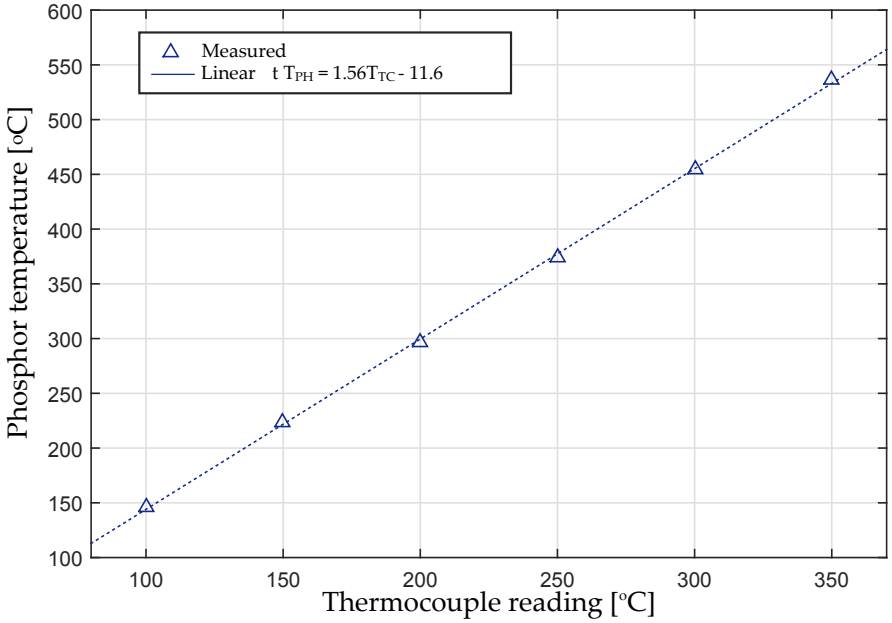

Figure 20: Measured temperature for position C3 and with an absolute pressure of 941 mbar with a flow of argon of 400 ml/min. The dotted line corresponds to the linear fit to the data points. T_{PH} is the temperature of the phosphor and T_{TC} is the thermocouple reading.

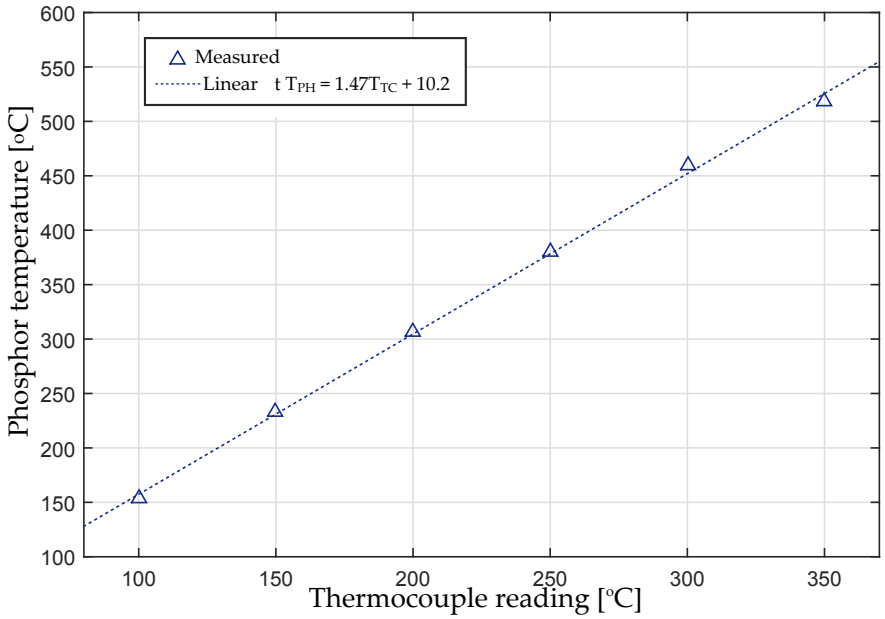

Figure 21: Measured temperature for position C3 and with an absolute pressure of 142 mbar with a flow of nitrogen of 100 ml/min. The dotted line corresponds to the linear fit to the data points. T_{PH} is the temperature of the phosphor and T_{TC} is the thermocouple reading.

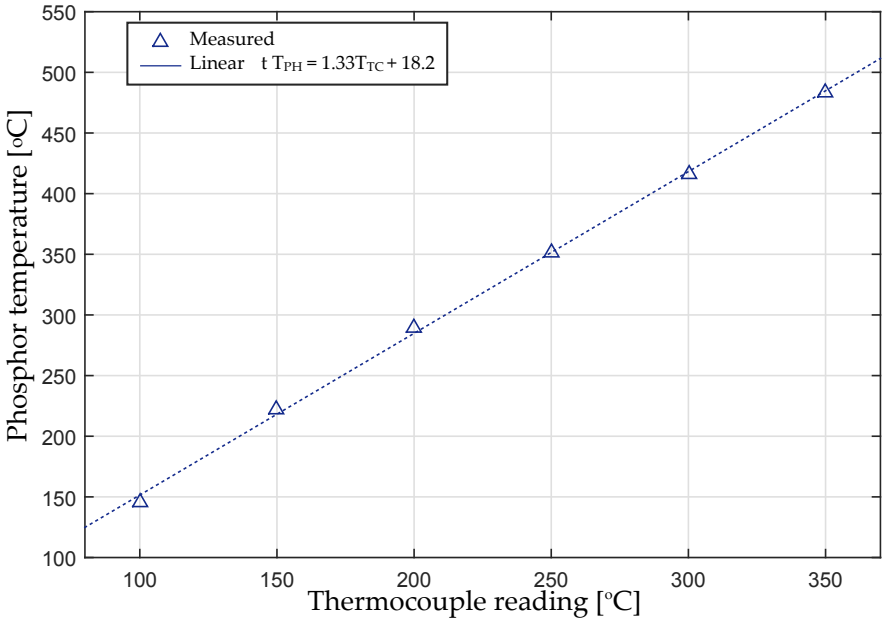

Figure 22: Measured temperature for position C5 and with an absolute pressure of 152 mbar with a flow of argon of 100 ml/min. The dotted line corresponds to the linear fit to the data points. T_{PH} is the temperature of the phosphor and T_{TC} is the thermocouple reading.

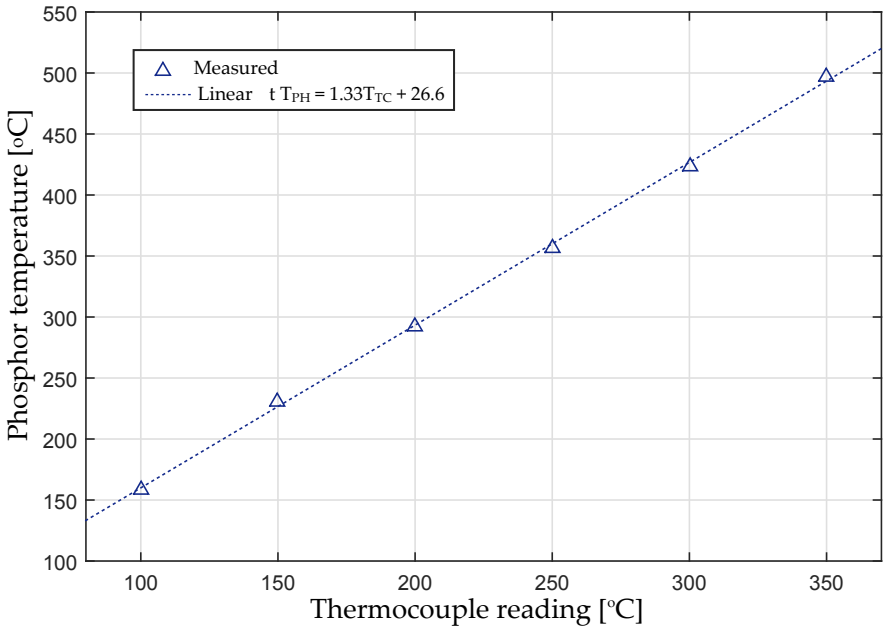

Figure 23: Measured temperature for the 10x10mm-sample at position S2C3, with an absolute pressure of 152 mbar with a flow of argon of 100 ml/min. The dotted line corresponds to the linear fit to the data points. T_{PH} is the temperature of the phosphor and T_{TC} is the thermocouple reading.

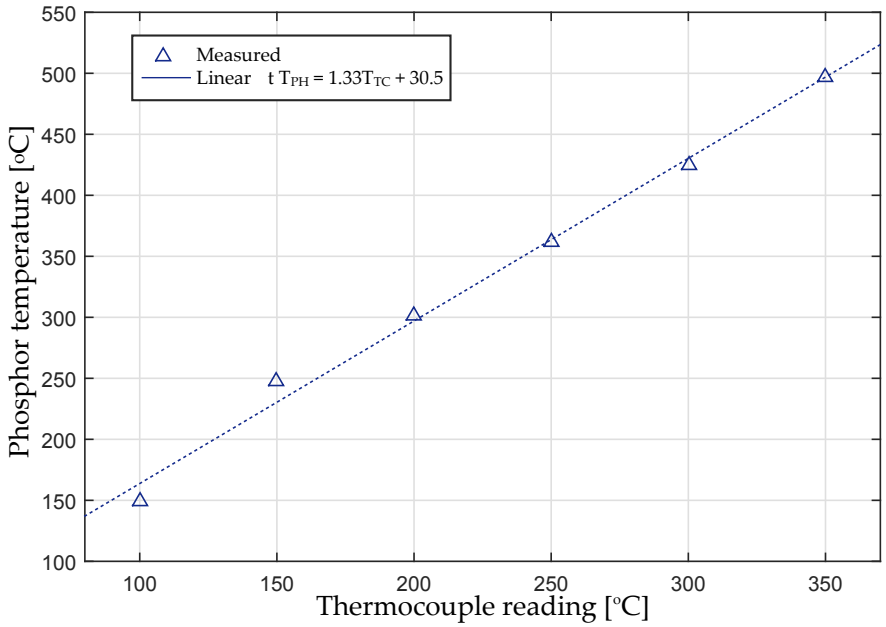

Figure 24: Measured temperature for the 4x4mm-sample at position S1C3, with an absolute pressure of 151 mbar with a flow of argon of 100 ml/min. The dotted line corresponds to the linear fit to the data points. T_{PH} is the temperature of the phosphor and T_{TC} is the thermocouple reading.

7 Appendix B: Photographs

This appendix contains photographs taken of the measurement equipment.

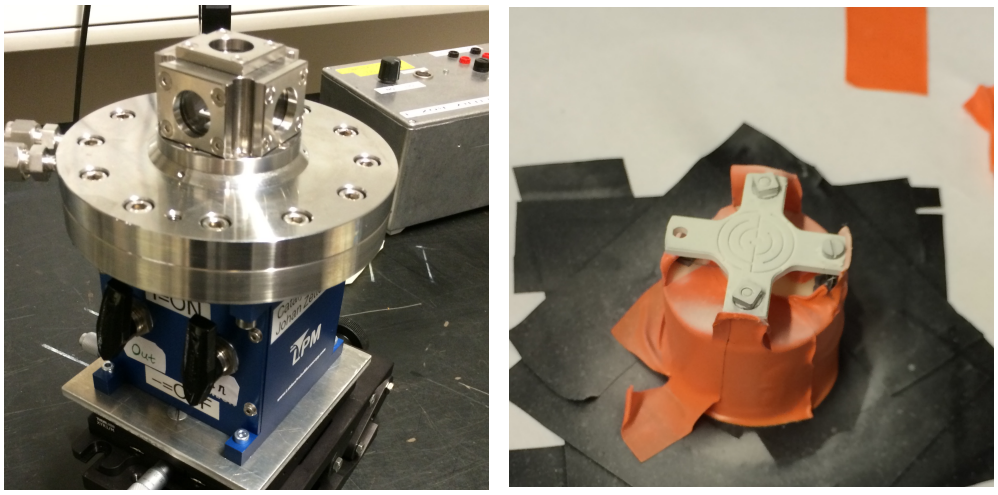

(a) Reaction chamber. **(b)** Sample holder.

Figure 25: Photographs of the reaction chamber and the phosphor-coated sample holder.

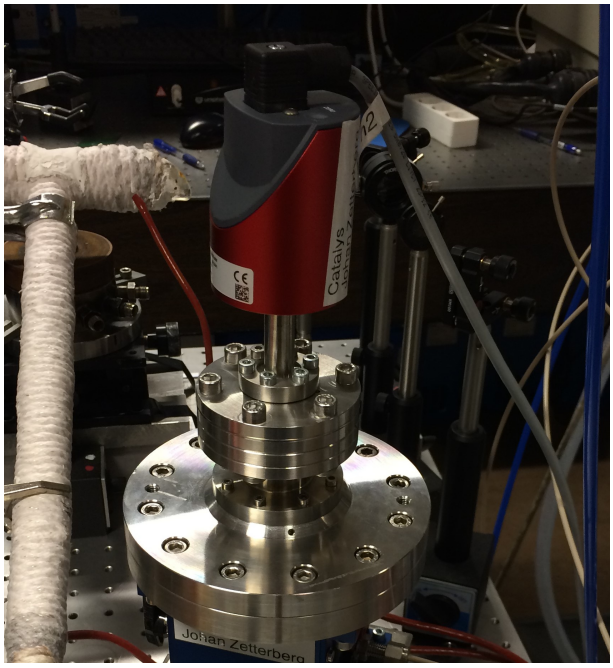

Figure 26: Photograph of one of the pressure gauges used in the measurements. The photograph shows the pressure gauge attached to the reaction chamber.